Quantitative Assessment of Upper-Limb Motor Function for Post-Stroke Rehabilitation Based on Motor Synergy Analysis and Multi-Modality Fusion

Chen Wang, Liang Peng, Zeng-Guang Hou, *Fellow, IEEE*, Jingyue Li, Tong Zhang, and Jun Zhao

***Abstract*— Functional assessment is an essential part of rehabilitation protocols after stroke. Conventionally, the assessment process relies heavily on clinical experience and lacks quantitative analysis. In order to objectively quantify the upper-limb motor impairments in patients with post-stroke hemiparesis, this study proposes a novel assessment approach based on motor synergy quantification and multi-modality fusion. Fifteen post-stroke hemiparetic patients and fifteen age-matched healthy persons participated in this study. During different goal-directed tasks, kinematic data and surface electromyography (sEMG) signals were synchronously collected from these participants, and then motor features extracted from each modal data could be fed into the respective local classifiers. In addition, kinematic synergies and muscle synergies were quantified by principal component analysis (PCA) and *k* weighted angular similarity (*k*WAS) algorithm to provide in-depth analysis of the coactivated features responsible for observable movement impairments. By integrating the outputs of local classifiers and the quantification results of motor synergies, ensemble classifiers can be created to generate quantitative assessment for different modalities separately. In order to further exploit the complementarity between the evaluation results at kinematic and muscular levels, a multi-modal fusion scheme was developed to comprehensively analyze the upper-limb motor function and generate a probability-based function score. Under the proposed assessment framework, three types of machine learning methods were employed to search the optimal performance of each classifier. Experimental results demonstrated that the classification accuracy was respectively improved by 4.86% and 2.78% when the analysis of kinematic and muscle synergies was embedded in the assessment system, and could be further enhanced to 96.06% by fusing the characteristics derived from different modalities. Furthermore, the assessment result of multi-modality fusion framework exhibited a significant correlation with the score of standard clinical tests ($R = -0.87$, $P = 1.98e-5$). These promising results show the feasibility of applying the proposed method to clinical assessments for post-stroke hemiparetic patients.**

***Index Terms*— Post-stroke hemiparesis, upper limb functional assessment, motor synergies, multi-modality fusion, motion capture technology, electromyography (EMG).**

I. Introduction

STROKE is a chronic disease induced by cerebral haemorrhage or infarction, and is one of the most frequent etiologies of non-traumatic disability in humans [1], [2]. Approximately two thirds of post-stroke patients have severe deficits in upper-limb movements, which affect their performance in ADLs (activities of daily living) [3]. In order to help these patients regain the motor function to some extent, long-term and high-intensity rehabilitation (i.e. physical therapy and occupational therapy) are considered essential, and motor function assessment plays an important role in the rehabilitation process. The assessment step is used to establish a baseline and individualize the directions of interventions at the beginning of rehabilitation, and the same assessment is focus on evaluating the treatment efficacy once therapeutic interventions have been initiated [4].

In general, upper-limb function assessment is manually performed by therapists using observation-based measures, such as Brunnstrom recovery stage [5], Fugl-Meyer assessment [6] and modified Ashworth scale [7]. The evaluation outcomes of these conventional assessment methods rely heavily on

Manuscript received September 23, 2019; revised December 28, 2019 and February 23, 2020; accepted February 25, 2020. Date of publication March 4, 2020; date of current version April 8, 2020. This work was supported in part by the National Natural Science Foundation of China under Grant 61720106012, Grant 61603386, Grant U1613228, and Grant U1913601, in part by the Beijing Natural Science Foundation under Grant L172050 and Grant Z170003, and in part by the Strategic Priority Research Program of Chinese Academy of Science under Grant XDB32040000. *(Corresponding author: Zeng-Guang Hou.)*

Chen Wang is with the State Key Laboratory of Management and Control for Complex Systems, Institute of Automation, Chinese Academy of Sciences, Beijing 100190, China, and also with the School of Artificial Intelligence, University of Chinese Academy of Sciences, Beijing 100049, China (e-mail: wangchen2016@ia.ac.cn).

Liang Peng is with the State Key Laboratory of Management and Control for Complex Systems, Institute of Automation, Chinese Academy of Sciences, Beijing 100190, China (e-mail: liang.peng@ia.ac.cn).

Zeng-Guang Hou is with the State Key Laboratory of Management and Control for Complex Systems, Institute of Automation, Chinese Academy of Sciences, Beijing 100190, China, also with the School of Artificial Intelligence, University of Chinese Academy of Sciences, Beijing 100049, China, and also with the CAS Center for Excellence in Brain Science and Intelligence Technology, Beijing 100190, China (e-mail: zengguang.hou@ia.ac.cn).

Jingyue Li, Tong Zhang, and Jun Zhao are with the China Rehabilitation Research Center, Beijing Bo'ai Hospital, Beijing 100068, China (e-mail: lijingyue87@126.com; tom611@126.com; zaojun@aliyun.com).

Digital Object Identifier 10.1109/TNSRE.2020.2978273

clinical experience and hence inevitably tend to be subjective [8]. In addition, the lack of quantitative and sensitive upper-limb movement analysis is also the limitation of the conventional methods. Therefore, there is considerable interest in developing an automated system to achieve objective and quantitative assessments for post-stroke rehabilitation.

Over the recent twenty years, human motion measuring and analysis have made significant progress, which provide technical foundations for the automation of upper-limb function assessment. Most previous studies have taken traditional clinical tests as the design references, and utilized motion capture technology to acquire upper-limb kinematics [9], [10]. Such approaches have an important limitation due to the ignorance of the intrinsic muscle activity responsible for the extrinsic arm movements. More concretely, muscle activation patterns in post-stroke patients have been demonstrated to be weak and delayed in amplitude, which lead to the abnormal patterns in observable movements [11]. Hence, to truly improve the sensitivity and reliability of functional evaluation, both kinematic and muscular characteristics should be emphasized in the construction of assessment systems.

By considering that stroke survivors frequently suffer from abnormal couplings between shoulder and elbow movements, pathological synergies can be regarded as markers of patients' functional status [12]. The concept of 'synergy' is originally used to describe the resolution determined by central nervous system (CNS) to overcome the redundancy of the musculoskeletal system [13]. For post-stroke hemiparetic patients, the flexion synergy and extension synergy frequently emerge before isolated upper-limb movements, and there are evidences that these pathological kinematic synergies are the results of altered coactivation of muscles [14], [15]. Addressing the points above, Cheung *et al.* [16] and Clark *et al.* [17] identified the muscle synergies to evaluate upper-limb motor impairment and locomotor performance respectively. Similar approaches are presented in [18], where muscular features sensitive to the multiple sclerosis disease are extracted. Specifically, matrix factorization algorithms are commonly applied for motor synergy analysis (e.g. principal component analysis (PCA), non-negative matrix factorization (NMF) and independent component analysis (ICA)) [19]–[21]. To our knowledge, the quantitative analysis of kinematic and muscle synergies has seldom been collectively incorporated into upper-limb function assessment systems.

Furthermore, in order to automatically distinguish between pathological and normal movement patterns, pattern recognition techniques play a major role in assessment systems, which can learn a relationship between features extracted from movement measurements and the corresponding clinical diagnosis. There have been a number of studies applying such methods for the automated assessment of upper-limb motor function, e.g., neural network [10], support vector machine [22], decision tree [23] and random forest [24]. However, these studies only qualitatively classify pathological patterns into several categories, and are largely confined to single-modal characteristics (e.g. kinematics), which cannot provide comprehensive diagnosis of upper extremity functional status.

In this study, we introduce a novel assessment approach to objectively quantify the upper-limb motor function of post-stroke hemiparetic patients. Kinematic data and surface electromyography (sEMG) signals were synchronously recorded during the feasible yet challenging goal-directed tasks. For each modality, motor features were statistically extracted and motor synergies were quantitatively analyzed to construct the single-modality classifier. Furthermore, the complementarity between the evaluation outcomes from different modalities was exploited by a multi-modal fusion scheme to provide more comprehensive assessment of upper extremity functional status. Under the proposed assessment framework, the pathological movement patterns in patients with post-stroke hemiparesis can be reliably identified and the assessment result is well correlated with the score of traditional clinical tests.

The main contributions of the paper are:

- An experimental platform was designed to elicit different goal-directed movements, which can ensure the participation of upper-limb muscles and joints.
- Kinematic and muscle synergies were quantified to characterize the altered coactivated features responsible for observable movement disorders. To the best of our knowledge, this is the first study to integrate the analysis of kinematic and muscle synergies for upper-limb function assessment.
- Three types of machine learning algorithms were adopted in the multi-modality fusion framework, including kernel-based machine learning algorithm, neural network and ensemble learning algorithm.
- A novel function score was automatically generated to reflect the degree of upper-limb motor impairment, which can be utilized as a reliable marker of upper extremity functional status.

The remaining parts of this study are organized as follows: Section II introduces our experimental set-up and the acquisition of multi-modal data. Section III details the assessment framework based on motor synergy quantification and multi-modal data fusion. Then experimental results are presented in Section IV, and Section V discusses the results. Finally, Section VI concludes the paper.

II. Experimental Methods

A. Participants

Our experiments were conducted in collaboration with China Rehabilitation Research Center (Beijing Bo'ai Hospital), and recruited fifteen post-stroke hemiparetic patients (9 males, 6 females, mean age 52.1 $\pm$ 15.1 years) from the hospital. Fifteen healthy subjects (10 males, 5 females, mean age 48.5 $\pm$ 13.1 years) were included for comparison.

The inclusion criteria for patients selection included: 1) the subject has experienced a first-ever ischemic or hemorrhagic stroke; 2) unilateral hemispheric lesions of the dominant side revealed by computed tomography or magnetic resonance imaging; 3) no major post-stroke complication; 4) no severe cognitive deficits; 5) able to accomplish unsupported upper-limb reaching movements (at Brunnstrom Stages III and

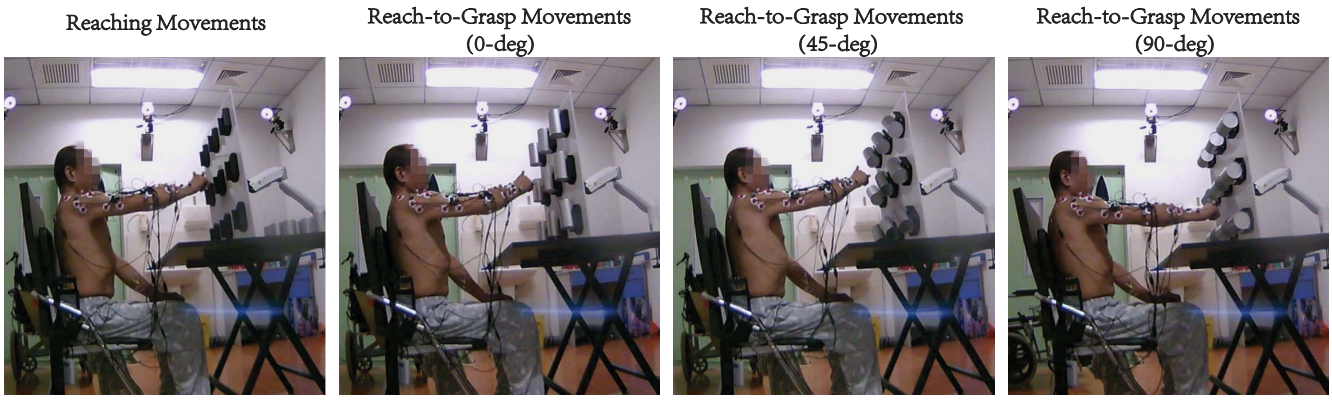

Fig. 1. Illustration of the experimental setup: the participant performed four types of goal-directed movements successively. The handles for grasping were respectively oriented at 0°, 45°, 90° relative to the direction of gravity for different reach-to-grasp tasks, which benefits the analysis of motor synergies in various arm postures.

TABLE I
DEMOGRAPHIC AND CLINICAL CHARACTERISTICS OF PATIENTS WITH POST-STROKE HEMIPARESIS

Age/Sex	Etiology	Side	BRS	FMA	MAS
49/F	Ischemic	Left	IV	56	1
75/F	Ischemic	Right	III	27	1+
41/F	Hemorrhagic	Left	III	42	2
34/M	Ischemic	Left	III	33	1+
73/F	Ischemic	Left	IV	45	1
57/M	Ischemic	Right	VI	60	0
53/F	Hemorrhagic	Right	VI	61	0
73/F	Ischemic	Left	III	30	1
60/M	Hemorrhagic	Left	V	58	0
32/M	Ischemic	Right	VI	52	1
37/M	Ischemic	Left	III	29	1
62/M	Ischemic	Left	V	60	0
61/M	Ischemic	Right	III	43	1
35/M	Ischemic	Right	III	35	1+
40/M	Ischemic	Left	IV	50	1

* BRS = Brunnstrom Recovery Stage, FMA = Fugl-Meyer Assessment, MAS = Modified Ashworth Scale; All standard clinical tests are carried out for the upper extremity of the impaired side.

above). Prior to the experiment, each post-stroke participant was examined by an experienced therapist for the Brunnstrom stage classification, the upper extremity section of Fugl-Meyer assessment, and the modified Ashworth scale. The clinical characteristics of the patients are presented in Table I.

The inclusion criteria for control subjects were able-bodied, and no history of neurological or musculoskeletal-related disability. Considering the differences between motor behaviours of dominant and non-dominant arms, we enrolled eight right-hand dominant and seven left-hand dominant healthy persons for controlled experiments. This research was reviewed and approved by the Ethics Committee of China Rehabilitation Research Center (approval number: 2017-096-1). Written informed consent was signed by each subject prior to inclusion in the study.

B. Experimental Equipment and Data Acquisition

We have developed a novel experimental platform with the aim to elicit various goal-directed movements. Nine rotatable cups (height 12 cm, diameter 6.5 cm) were fixed on the plate by magnets positioned within recesses, and served as the targets for reaching or reach-to-grasp movements. The platform was fixed to a table, and the workspace was located at a distance from the participant according to 90% of the maximum reach. The height of the workspace was individually adjusted to guarantee that the center of the plate was aligned with the corresponding shoulder of the participant (Fig. 1).

In order to explore the kinematic and muscular characteristics in normal and pathological movement patterns, kinematic and electrophysiological data were collected synchronously in all experiments. The kinematic data was recorded by an optical motion tracking system (Qualisys AB, Gothenburg, Sweden) at a sampling rate of 200 Hz, which consists of 6 high-speed CCD cameras. Specifically, eleven reflective markers were attached to participants' upper extremities at anatomical positions (Fig. 2). In addition, ten-channel sEMG signals were acquired at 1000 Hz using a ME6000 Biomonitor (Mega Electronics Ltd., Kuopio, Finland). Thirty sEMG electrodes were attached to ten major muscles according to the anatomical locations of human muscles (Fig. 2). The above acquisition processes of multi-modal data were synchronized via Qualisys Track Manager Software (Qualisys, Sweden).

C. Experimental Protocol

The ability to reach and grasp objects is the basis for most ADLs, such as feeding, grooming and other behaviors. Post-stroke patients often have difficulty with the control of such goal-oriented movements, and the severity of motor impairments depends on how much the cerebral tissue is damaged [25]. In order to comprehensively assess upper-limb motor function, four experimental tasks were designed in this study, including one reaching task and three reach-to-grasp tasks. Patients with post-stroke hemiparesis were instructed to perform the tasks with their impaired arm, and healthy participants used their dominant arm to accomplish the tasks. By considering post-stroke patients commonly employ trunk movements to compensate for the upper-limb motor deficits [14], all the experiments were carried out under the guidance of an experienced therapist, with the aim to limit the compensatory trunk movements of patients.

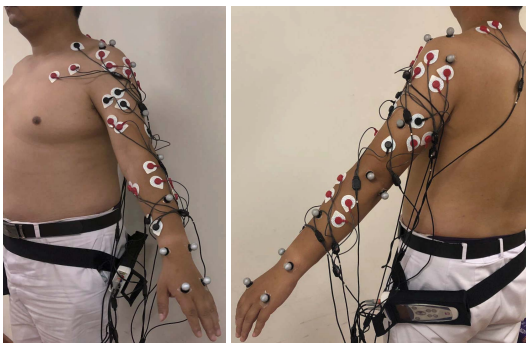

Fig. 2. The placement of eleven reflective markers: acromion, head of humerus, superior angle of scapula, medial edge of the humerus, head of radius, olecranon, medial edge of the forearm, styloid process of radius, styloid process of ulna, second metacarpal bones, and fifth metacarpal bones. Surface electrodes placement for ten major muscles: pronator teres, biceps brachii long head, triceps brachii lateral head, deltoid anterior head, deltoid middle head, deltoid posterior head, pectoralis major, upper trapezius, brachioradialis, and extensor digitorum.

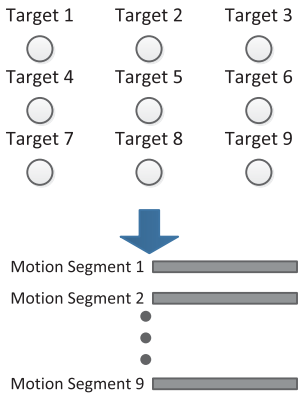

Fig. 3. Demonstration of motion segmentation: the onset of a motion segment towards a specified target was defined as the time when the hand velocity exceeded 0.05 m/s, and the termination was defined as the time when the hand returned to the starting position. The motion segment comprised the corresponding multi-modal data.

For the reaching task, the participant was asked to point each target with index finger, and the sequence of targets is depicted in Fig. 3. For the reach-to-grasp tasks, the orientations of handles were 0°, 45°, 90° with respect to the direction of gravity, respectively. Similar to the reaching task, the participant was instructed to make reaching movements and grasp handles in a comfortable posture. In the initial posture, the participant was seated in a high back chair with hips and knees flexed 90°, and rested the impaired/ dominant arm at the starting position on the table. Within each task, after a 'go' signal given by the experimenter, the participant initiated reaching or reach-to-grasp movements, pointed or grasped the specified target, and returned to the starting position empty-handed. Once returning to the initial posture, the participant performed the similar movements for the next target (a total of nine targets). A complete trial consists of the successive accomplishment of one reaching task, one reach-to-grasp task (0°), one reach-to-grasp task (45°) and one reach-to-grasp task (90°). It is worth noting that each participant was required to perform at least one successful trial (Fig. 1).

D. Data Preprocessing

1) Kinematic Data: As the human arm can be simplified as a kinematic chain with three segments, an upper limb model with seven Degrees-of-Freedoms (DOFs) was built, and the joint angles for seven primary motions were calculated: shoulder internal/external rotation, shoulder flexion/extension, shoulder adduction/abduction, elbow flexion/extension, wrist supination/pronation, wrist flexion/extension, and wrist radial/ulnar deviation. Considering that the characteristics of human arm redundancy resolution can be mathematically represented by a swivel angle [26], we also calculated the swivel angle for kinematic analysis. The mathematical calculations are detailed in our previous study [27].

2) Electrophysiological Data: As the industrial frequency noise has already been eliminated by electrodes, the ten-channel sEMG signals were band-pass filtered from 20 to 200 Hz to remove DC offset and high-frequency noise, and then were full-wave rectified. In order to eliminate high-frequency noise introduced by full-wave rectification, a low-pass Butterworth filter with cutoff frequency 5 Hz was adopted. After obtaining the smooth envelopes of sEMG signals, we normalized the envelope of each muscle for each participant by its maximum sEMG amplitude obtained over all tasks, and then aligned the sampling frequency of muscle activity with that of kinematic data. Details on the calculation of sEMG signals can be found in [18].

3) Motion Segmentation: In four experimental tasks, the onset of the goal-directed movement was defined as the time when the magnitude of hand markers velocities exceeded 0.05 m/s, and the end of movement was identified as the moment when the hand returned to the starting position. Thus, the duration of the movement towards a specified target was the time interval between the above events, and small oscillations at the movement onset and termination were not included. To provide more accurate information of upper-limb movement disorders, the preprocessed kinematic and electrophysiological data were separately segmented into nine segments for each experimental task (Fig. 3). Hence, for every individual, there are 4*9 = 36 motion segments for each modality.

III. Multi-Modality Fusion Framework for Functional Assessment

A. Extraction of Statistical Motor Features

As most stroke survivors are left with defective control of global movements (e.g. reaching) accompanied by spasticity, motor features extracted from kinematic and muscular levels can be used to characterize movement disorders.

For the kinematic level, numerous observations have demonstrated that the point-to-point movements performed by healthy persons in unconstrained situations comply with the minimum-jerk principle [28], [29], which tends to maximize the movement smoothness. The minimum-jerk trajectory from (x_i, y_i, z_i) to (x_d, y_d, z_d) can be expressed in the following

form:

$$\begin{aligned} x(t) &= x_i + (x_d - x_i)\left(10\tau^3 - 15\tau^4 + 6\tau^5\right) \\ y(t) &= y_i + (y_d - y_i)\left(10\tau^3 - 15\tau^4 + 6\tau^5\right) \\ z(t) &= z_i + (z_d - z_i)\left(10\tau^3 - 15\tau^4 + 6\tau^5\right), \end{aligned} \tag{1}$$

where t_d is the total time of the goal-directed movements, and $\tau = t/t_d$. Therefore, two standard minimum-jerk trajectories were generated for a motion segment, i.e., one trajectory from the starting position to the target and the other trajectory in the opposite direction. The time-varying deviation between the actual trajectory of wrist movements X_a and the standard trajectory X_s was calculated for each direction in a motion segment:

$$\tilde{X} = X_a - X_s, \tag{2}$$

where $X = [x, y, z]^T$ is defined in the three-dimensional Cartesian coordinate system.

Then statistical analysis was executed to extract the mean value (MV) and standard deviation (SD) from $\tilde{X}$:

$$MV_d = \frac{1}{N}\sum_{k=1}^{N}\tilde{X}_k \tag{3}$$

$$SD_d = \sqrt{\frac{1}{N-1}\sum_{k=1}^{N}(\tilde{X}_k - MV_d)^2}, \tag{4}$$

where k is the sample index, and N is the sample size of the motion segment.

In order to characterize the oscillations of elbow joint, wrist joint and hand, the difference absolute mean value (DAMV) was also used as a statistical motor feature, and the calculation can be expressed as:

$$DAMV = \frac{1}{N-1}\sum_{k=2}^{N}|X_k - X_{k-1}|, \tag{5}$$

where $DAMV_e$ represents the average displacement between two adjacent position of elbow joint, similarly, $DAMV_w$ and $DAMV_h$ are calculated from the coordinate sequences of wrist joint and hand, respectively.

For the muscular level, in order to assess the impairments in muscle activity responsible for the observable postural control deficits, the mean absolute value (MAV) was extracted from ten-channel sEMG signals, which is one of the most prominent features used in sEMG signal analysis and can be defined as:

$$MAV_m = \frac{1}{N}\sum_{i=1}^{N}|u_i|, \tag{6}$$

where u_i is the ith data point of the sEMG sequence, and N is the number of samples in the motion segment. In addition, the standard deviation feature of sEMG signals (SD_m) was calculated to serve as another statistical feature.

B. Quantification of Upper-Limb Synergies

In order to quantify the coactivated features at kinematic and muscular levels, we identified upper-limb synergies involved in the goal-directed movements. To begin with, the joint angle time courses were constituted by the joint kinematics derived in Section II-D, and then the correlation matrix was calculated based on the angular time courses of each motion segment to guarantee the equal weight of each observed variable. PCA was performed by finding the eigenvectors and eigenvalues of the correlation matrix with the aim to transform seven DOFs into a set of uncorrelated linear combinations or PCs. Therefore, kinematic synergies can be characterized mathematically by a set of PCs.

In this study, instead of computing PCs, we compared the subspace spanned by the set of PCs by obtaining the angular similarity between the eigenvectors that uncover how much each joint angle contributes to each PC. The difference between the pathological and normal kinematic synergies can be quantified according to kWAS algorithm [30]:

$$\psi\left(S_p, S_h\right) = 1 - \frac{1}{2}\sum_{i=1}^{n}\left[\left(\frac{\sigma_i}{\sum_{j=1}^{n}\sigma_j} + \frac{\lambda_i}{\sum_{j=1}^{n}\lambda_j}\right)|u_i \cdot v_i|\right] \tag{7}$$

where σ_i and λ_i are the ith eigenvalues corresponding to the eigenvectors u_i and v_i of two different correlation matrices, respectively. For the evaluation of altered joint coordination, S_p and S_h represent the kinematic synergies extracted from a single participant and the healthy control group, respectively. $n = 7$ retains all coactivation patterns of seven DOFs in computation.

Furthermore, PCA was similarly carried out on ten-channel sEMG signals to yield the eigenvectors and eigenvalues of each motion segment. The impairments in muscle synergies can be quantitatively described by solving the equation 7. Specifically, S_p and S_h denotes the muscle synergies of an individual participant and the healthy control group, respectively. $n = 10$ represents that all synergies extracted from ten major muscles are involved in the comparison.

In summary, ψ_k and ψ_m were respectively defined to characterize differences in upper-limb synergies between post-stroke hemiparetic patients and healthy persons at kinematic and muscular levels (Fig. 4). As the value of ψ ranges over [0, 1] and become larger when the abnormality is more severe, ψ_k and ψ_m can provide deep-seated evaluation of upper-limb motor ability.

C. Single-Modality Classifier

After statistical feature extraction and motor synergy quantification, two types of single-modality classifiers (i.e. local classifiers and ensemble classifiers) were created to evaluate upper-limb motor function based on the characteristics derived from each modal data (Fig. 4).

In this study, we adopted three types of supervised machine learning methods to build the candidate single-modality classifiers, consisting of SVM, BPNN and RF. The SVM classifier with radial basis function (RBF) kernel served as a

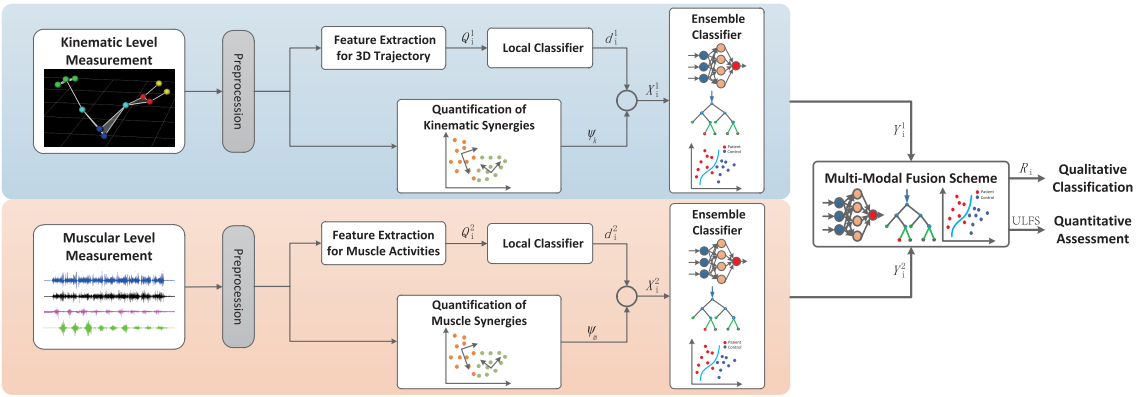

Fig. 4. The assessment framework based on motor synergy quantification and multi-modal data fusion.

representative of the kernel-based machine learning algorithm, and Platt's method [31] was utilized to estimate the posterior probabilities from outputs. The BPNN classifier was defined as a feedforward neural network comprising three layers, and the output layer selected sigmoid function as the activation function. To optimize the weights and biases, the gradient descent algorithm was employed in the neural network. The RF classifier can be considered as the ensemble learning algorithm in essence, thus the classification result was decided by the majority vote of decision trees.

An experimental sample was defined as the multi-modal data synchronously collected in a motion segment, and the corresponding ground truth label was determined according to the group of the participant (+1 for pathological group and −1 for healthy group). For the local single-modality classifier, the input vector Q_i^m extracted from the mth modality of the ith motion segment was uniformly defined as:

$$Q_i^m = \left[v_1^m, \cdots, v_n^m, \cdots, v_{N_l^m}^m\right]^T, \tag{8}$$

where v_n^m is the nth statistical motor features, N_l^m is the total number of selected features; Q_i^1 and Q_i^2 represent the input vectors of the kinematics-based and sEMG-based local classifiers, respectively. The feature vectors of different modalities were subsequently imported into their respective classifiers, and the output vector of mth modality can be obtained:

$$d_i^m = f_{local}^m(Q_i^m), \tag{9}$$

where f_{local}^m denotes three candidate classifiers based on supervised classification algorithms, and d_i^m is the corresponding predicted probability of the sample belonging to the pathological group.

Then the outputs of local single-modality classifiers were integrated with the evaluation outcomes of upper-limb synergies to construct the input vectors of ensemble single-modality classifiers, which can be further expressed as:

$$X_i^m = [\eta_1^m, \cdots, \eta_n^m, \cdots, \eta_{N_e^m}^m]^T, \tag{10}$$

where X_i^m represents the feature vector extracted from the ith motion segment which fed to the candidate ensemble classifiers of the mth modality, and η_n^m denotes the combination of local decisions and coactivated features. Consequently, the predicted results of three types of candidate classification models were uniformly represented as:

$$Y_i^m = f_{ensemble}^m(X_i^m), \tag{11}$$

where Y_i^m is the predicted probability vector of the ith motion segment, hence the final result for single-modal assessment can be determined.

More concretely, the constitution of input vector for each modality is worthy of note:

- For the kinematic level, the statistical features of trajectory deviation (MV_d and SD_d), as well as the vibration amplitudes ($DAMV_e$, $DAMV_w$ and $DAMV_h$) were selected to constitute the input vector fed to the local classifier. Further, the input vector of the ensemble classifier was composed of the local output (d_i^1), the quantification of kinematic synergies (ψ_k), and statistical features of swivel angle (MV and SD).
- For the muscular level, the integration of MAV_m and SD_m extracted from ten-channel sEMG signals was utilized as the input vector of the local classifier to distinguish pathological and normal patterns in muscle activity. Based on the local output (d_i^2), the input vector of ensemble classifier was constructed by incorporating the quantification of muscle synergies (ψ_m).

D. Multi-Modal Fusion Scheme

As the quantitative functional assessment was achieved at kinematic and muscular levels separately, a multi-modal fusion scheme was proposed to make the best use of the ensemble outputs of different modalities in this stage (Fig. 4). Kernel-based classification algorithm (SVM), artificial neural network method (BPNN), and ensemble learning algorithm (RF) were employed in the fusion scheme.

To comprehensively analyze the upper-limb motor function in patients with post-stroke hemiparesis, the outputs of the selected ensemble classifiers were concatenated together to form the input vector of the fusion model, which can be expressed as:

$$R_i = G_{fusion}(Y_i^1, \cdots, Y_i^m, \cdots, Y_i^M), \tag{12}$$

where R_i is the final predicted probability of the ith motion segment, G_{fusion} denotes the fusion algorithm, and Y_i^m has been defined in equation 11.

TABLE II
OVERALL ACCURACY (%), PRECISION (%), RECALL (%) AND F1-MEASURE (%) OF KINEMATICS-BASED CLASSIFIERS

Performance Measures	Local Classifier			Ensemble Classifier		
	SVM	BPNN	RF	SVM	BPNN	RF
Accuracy	87.96	84.72	86.57	92.82	88.19	88.66
Precision	97.89	99.24	97.16	99.00	98.92	99.64
Recall	85.80	80.25	84.57	91.36	85.19	85.19
F1-Measure	91.45	88.74	90.43	95.02	91.54	91.85

As the value of R_i can provide the possibility that the motion segment belongs to a certain class, the qualitative classification was achieved by automatically assigning the motion segment to the class with higher possibility. Furthermore, the probabilities of 36 samples from an individual participant were fused to constitute a quantitative assessment score, which named as upper-limb function score (ULFS). It can be verified that the ULFS quantitatively represents the upper-limb functional status of an individual participant as a number ranging from 0 to 36. As the value of ULFS becomes lower when the upper-limb motor ability approaches normal status, the quantitative assessment of upper-limb motor function can be achieved in patients with hemiparesis.

The training strategy of the multi-modal framework can be summarized in the following steps. To begin with, the multi-modal data collected in 1080 motion segments extracted from the movements of 30 participants served as the full dataset, which was randomly divided into the training and test set (60% and 40% of the dataset). In order to achieve effective training of the three-layer model, the training set needed to be split into three non-overlapping parts (40%, 30% and 30% of the training set). Then the first training part and corresponding ground truth labels were utilized to construct the candidate local classifiers of each modality, and optimal classifier was selected according to classification performance by feeding the second training part to the above local classifiers. Subsequently, the outputs of optimal local classifiers were integrated with the quantification results of their respective synergies to build ensemble single-modality classifiers, and optimal ensemble classifiers could be similarly determined by the third training part. Finally, the predicted probabilities of these selected ensemble classifiers were concatenated together to form a feature vector, which served as the input of the multi-modal fusion model. The remaining 30% of the full dataset was utilized to test the performance of the assessment system. In addition, hyperparameters of classification models were selected by employing 5-fold cross validation procedures.

IV. RESULTS

A. Performance of Qualitative Classification

Once the proposed assessment framework was trained with multi-modal data and the corresponding ground truth labels, the qualitative classification ability of this framework can be generalized to the unknown data collected from goal-directed movements. In this study, accuracy, precision, recall and F1-measure were utilized to evaluate the classification performance. To further compare the ability of classifiers with different machine learning methods to accurately identify pathological movement patterns, receiver operating characteristic (ROC) curves [32] were plotted for all candidate classifiers, and the area under the ROC curve (AUC) values were calculated, which can be regarded as a composite measure of classification performance.

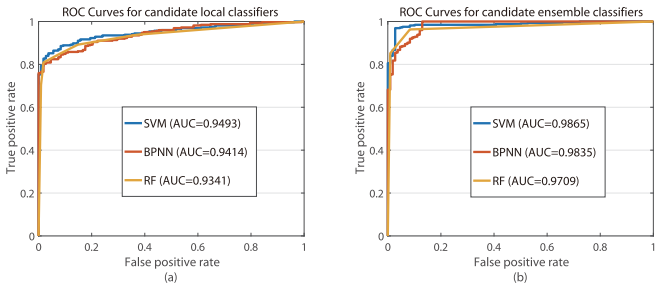

Fig. 5. ROC curves and AUC values for kinematics-based single-modality classifiers: (a) candidate local classifiers, (b) candidate ensemble classifiers. SVM produced the best performance in the construction of the local classifier and ensemble classifier. The analysis of kinematic synergies has a positive effect on classification performance.

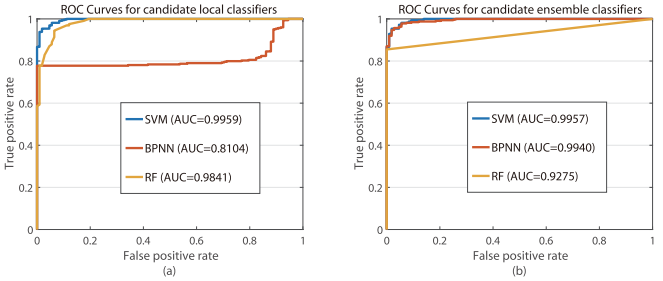

Fig. 6. ROC curves and AUC values for sEMG-based single-modality classifiers: (a) candidate local classifiers, (b) candidate ensemble classifiers. SVM and BPNN produced the best performance in the construction of the local classifier and ensemble classifier, respectively. The analysis of muscle synergies has a positive effect on classification performance.

For kinematics-based single-modality classifiers, we evaluated different supervised classification algorithms on the test set respectively, with the aim to test the optimal models of local and ensemble classifiers. The results in Table II show the classification performance of single-modality classifiers, and the optimal results of local and ensemble classifiers are respectively highlighted in pink and blue. With statistical motor features, SVM displayed an overall accuracy of 87.96% in local classification, which was higher than BPNN and RF by a margin of 3.24% and 1.39%, respectively. By integrating the output of the SVM classifier with the quantification result of kinematic synergies, SVM also achieved higher accuracy rate than BPNN and RF in ensemble classification, and attained better F1-measure. Fig. 5 further confirms the superior classification performance of SVM by demonstrating the greater ROC area in the local and ensemble classifiers. It is worth noting that the optimal classifiers selected by the test set were consistent with the results derived from the training set. In addition, the positive effect of kinematic synergies evaluation was demonstrated by comparing the best performance of local and ensemble classifiers (a 4.86% improvement).

TABLE III
OVERALL ACCURACY (%), PRECISION (%), RECALL (%) AND F1-MEASURE (%) OF SEMG-BASED CLASSIFIERS

Performance Measures	Local Classifier			Ensemble Classifier		
	SVM	BPNN	RF	SVM	BPNN	RF
Accuracy	87.96	83.33	86.11	89.35	90.74	89.12
Precision	100.0	100.0	98.89	100.0	99.65	100.0
Recall	83.95	77.78	82.41	85.80	87.96	85.49
F1-Measure	91.28	87.50	89.90	92.36	93.44	92.18

TABLE IV
OVERALL ACCURACY (%), PRECISION (%), RECALL (%) AND F1-MEASURE (%) OF MULTI-MODAL FUSION SCHEMES

Performance Measures	Fusion Model		
	SVM	BPNN	RF
Accuracy	96.06	93.98	94.21
Precision	99.68	100.0	99.67
Recall	95.06	91.98	92.59
F1-Measure	97.31	95.82	96.00

For sEMG-based single-modality classifiers, Table III summarizes performance of candidate classifiers on the test set, and the optimal models for local and ensemble classification are shown in pink and blue highlighted cells respectively. It can be seen that SVM attained the highest accuracy rate (87.96%) and the best F1-measure (91.28%) in local classification. Based on the predicted probability of the optimal local classifier, BPNN demonstrated good performance in the construction of the ensemble classifier, as the overall accuracy outperformed SVM and RF by a margin of 1.39% and 1.62%, respectively. The results were in agreement with the optimal classifiers obtained from the training set, i.e., SVM for local classification and BPNN for ensemble classification. Fig. 6 depicts the ROC curves of all candidate classifiers, and the AUC values indicate that the analysis of muscle synergies plays an important role in the assessment system.

Under the multi-modal fusion architecture, the classification performance of SVM, BPNN and RF was similarly tested in terms of accuracy, precision, recall and F1-measure. Table IV illustrates the performance of three fusion models, and the optimal fusion result is highlighted in blue. The results indicate that accuracy rates are consistently better compared with the single-modality classifiers for all classification algorithms. The ROC curves of fusion models are presented in Fig. 7, and the AUC values for SVM, BPNN and RF were 0.9982, 0.9749 and 0.9583, respectively. Results suggest that SVM performs superiorly to both BPNN and RF in the multi-modal fusion scheme and is capable of distinguishing pathological movement characteristics with significantly high accuracy.

In this study, the best accuracy for the optimal kinematics-based ensemble classifier (OKEC), optimal sEMG-based ensemble classifier (OSEC), and optimal fusion classifier (OFC) were 92.82 %, 90.74% and 96.06 %. Therefore, the classification accuracy of the OFC is improved by 3.24% and 5.32% compared with that of the OKEC and

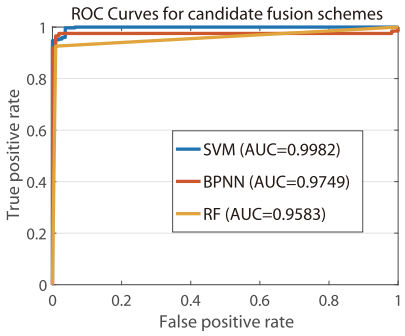

Fig. 7. ROC curves and AUC values for multi-modal fusion schemes. SVM produced the best performance in the multi-modal fusion scheme, which outperformed optimal single-modality classifiers.

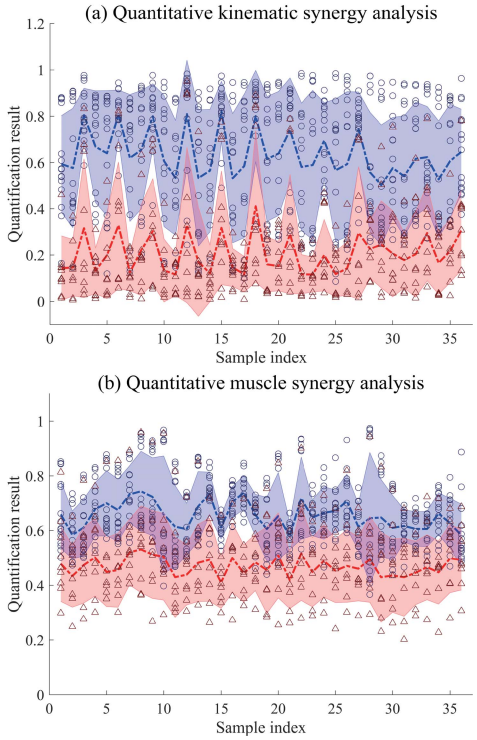

Fig. 8. Time-series quantification results of motor synergies for all participants: (a) kinematic synergies, (b) muscle synergies. Circular symbols and triangular symbols indicate the results derived from pathological group and healthy control group, respectively. The thick blue line and blue shaded zone represent the average evolution of quantification value and standard deviation across fifteen post-stroke hemiparetic participants. The thick red line and pink shaded zone represent the average evolution of quantification value and standard deviation across fifteen healthy participants.

OSEC, which suggests that upper-limb movement disorders of post-stroke hemiparetic patients can be reliably identified by integrating multi-modal characteristics.

B. Performance of Quantitative Assessment

Considering that the assessment system can identify pathological movements with considerably high accuracy, we further explored whether the proposed method can quantitatively analyze the upper-limb motor impairments in patients with post-stroke hemiparesis. As a first step, the quantitative assessment performance of kinematic or muscle synergy analysis

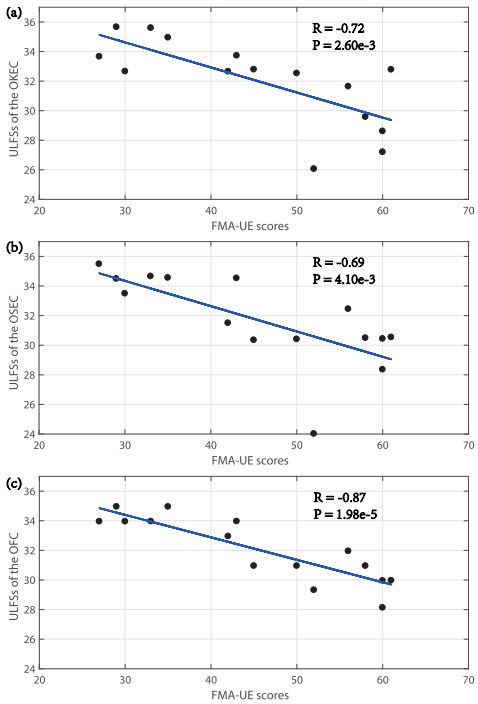

Fig. 9. Correlation analysis between the ULFSs and FMA-UE scores for the three optimal classifiers: (a) OKEC, (b) OSEC and (c) OFC. The Pearson correlation coefficient and the P-value (significance level $\alpha = 0.05$) are indicated in each subfigure, respectively.

was demonstrated by concatenating the values of ψ_k or ψ_m belonging to an individual participant, and the time-varying quantification results exhibited substantial differences between pathological and healthy control group during goal-directed movements (Fig. 8). Therefore, the quantification of kinematic and muscle synergies can provide objective evaluation of upper extremity functional status, specifically, a lower value indicates the better functional status and vice versa.

Furthermore, in order to validate the effectiveness of the quantitative assessment method, the OKEC, OSEC and OFC were taken as representatives to study consistency between the ULFS and the score of traditional assessment test. Since the Fugl-Meyer Assessment Upper Extremity (FMA-UE) score was obtained and a lower score indicates that the abnormality of upper-limb movements is more extensive (in the 0-66 range), Pearson correlation test [33] was carried out to analyze the correlation between the ULFS and the FMA-UE score with a significance level of 0.05. As can be seen, the ULFS derived from the OKEC showed a negative relationship with the FMA-UE score, but was not significant (R = −0.72, P = 2.60e-3, Fig. 9(a)). Similarly, we also found a trend to a negative correlation between the FMA-UE score and the ULFS derived from the OSEC (R = −0.69, P = 4.10e-3, Fig. 9(b)). The most significant correlation between two types of scores was achieved by the OFC, accompanied with the highest correlation coefficient (R = −0.87, P = 1.98e-5, Fig. 9(c)). Consequently, these promising results demonstrated that the integration of motor synergy analysis can be beneficial to quantitative assessment performance, and the multi-modal fusion scheme can improve the correlation coefficient and generate a more comprehensive assessment result to monitor the progression of motor recovery and evaluate the efficacy of the existing treatment.

V. Discussion

The main goal of this study is to develop an upper-limb assessment system for qualitative classification and quantitative analysis of motor impairment in patients with post-stroke hemiparesis. The system was constructed on the basis of kinematic data and sEMG signals collected synchronously during the feasible yet challenging goal-directed movements. Motor synergy quantification was conducted at kinematic and muscular levels, which provided in-depth analysis of coactivated features responsible for observable motor deficits. Under the multi-modal fusion framework, the quantitative assessment results of different modalities were integrated using supervised machine learning methods to realize objective and comprehensive assessment of upper-limb motor function.

For the analysis of motor synergies, most of the existing studies applied PCA to qualitatively evaluate pathological upper-limb synergies, such as the proportion of variance captured by each PC and the number of PC explaining most of the variance. The present study utilized PCA and kWAS algorithm to quantify kinematic and muscle synergies, and the results presented in Tables II and III suggest the advantage of embedding the quantification of upper-limb synergies in the assessment framework.

By exploiting the complementarity between the movement characteristics derived from different modalities, the results produced by the assessment system demonstrated that both the classification accuracy and clinical relevance can be enhanced. The system also generated a quantitative assessment score, which was well correlated with the score of standard clinical tests. From a clinical perspective, the exciting development is that the assessment process can be performed automatically and provides therapists with more time to modify rehabilitation protocols based on the assessment result.

Nonetheless, there are some limitations in the present study. Due to the fact that post-stroke patients at Brunnstrom Stages I and II can hardly perform unsupported upper-limb movements, our experiment design leads to that the proposed system can only provide evaluation for patients at Stages III and above. Therefore, the experimental task will be adjusted to meet the requirement of stroke survivors with more severe disability.

VI. Conclusion

This study presents an automated assessment system capable of fusing movement characteristics derived from kinematic data and sEMG signals, which has shown very encouraging performance in quantitative analysis of upper-limb movement disorders for post-stroke rehabilitation. The most important contribution of the proposed approach is the emphasis on both the observable motor features and the underlying coactivated features at kinematic and muscular levels. Experimental results of single-modality classifiers demonstrated that the quantification of motor synergies can be utilized as reliable markers to estimate upper extremity functional status in post-stroke hemiparetic patients. Further, the optimal multi-modal fusion

scheme exhibited superior performance in distinguishing pathological and normal movements with an overall accuracy of 96.06%, and its output showed a significant correlation with FMA-UE scores ($R = -0.87,\ P = 1.98e-5$). Given these promising results, the proposed assessment system has the potential to provide valuable information for clinical decision-making, as well as evaluate the effectiveness of treatment methods for post-stroke patients with upper limb hemiparesis. Future research will explore the establishment of rehabilitation strategies based on the assessment result to further validate the assessment system.

REFERENCES

[1] D. O'Neill, F. Horgan, A. Hickey, and H. McGee, "Stroke is a chronic disease with acute events," *BMJ*, vol. 336, no. 7642, p. 461, Feb. 2008.

[2] V. L. Feigin *et al.*, "Global and regional burden of stroke during 1990–2010: Findings from the Global Burden of Disease Study 2010," *Lancet*, vol. 383, no. 9913, pp. 245–255, 2014.

[3] G. E. Gresham, W. B. Stason, and P. W. Duncan, *Post Stroke Rehabilitation*. Diane Publishing, 2004, vol. 95, no. 662.

[4] M. Barnes, "Principles of neurological rehabilitation," *J. Neurol., Neurosurg. Psychiatry*, vol. 74, no. 4, pp. iv3–iv7, 2003.

[5] S. Brunnstrom, "Motor testing procedures in hemiplegia: Based on sequential recovery stages," *Phys. Therapy*, vol. 46, no. 4, pp. 357–375, Apr. 1966.

[6] A. R. Fugl-Meyer, L. Jääskö, I. Leyman, S. Olsson, and S. Steglind, "The post-stroke hemiplegic patient. 1. a method for evaluation of physical performance," *Scand. J. Rehabil. Med.*, vol. 7, no. 1, pp. 13–31, 1975.

[7] R. Bohannon and M. Smith, "Upper extremity strength deficits in hemiplegic stroke patients: Relationship between admission and discharge assessment and time since onset," *Arch. Phys. Med. Rehabil.*, vol. 68, no. 3, pp. 155–157, 1987.

[8] E. D. Ona Simbana, P. Sanchez-Herrera Baeza, A. Jardon Huete, and C. Balaguer, "Review of automated systems for upper limbs functional assessment in neurorehabilitation," *IEEE Access*, vol. 7, pp. 32352–32367, 2019.

[9] E. V. Olesh, S. Yakovenko, and V. Gritsenko, "Automated assessment of upper extremity movement impairment due to stroke," *PLoS ONE*, vol. 9, no. 8, Aug. 2014, Art. no. e104487.

[10] W.-S. Kim, S. Cho, D. Baek, H. Bang, and N.-J. Paik, "Upper extremity functional evaluation by fugl-meyer assessment scoring using depth-sensing camera in hemiplegic stroke patients," *PLoS ONE*, vol. 11, no. 7, Jul. 2016, Art. no. e0158640.

[11] S. J. Garland, V. L. Gray, and S. Knorr, "Muscle activation patterns and postural control following stroke," *Motor Control*, vol. 13, no. 4, pp. 387–411, Oct. 2009.

[12] T. E. Twitchell, "The restoration of motor function following hemiplegia in man," *Brain*, vol. 74, no. 4, pp. 443–480, 1951.

[13] G. Assal, "The co-ordination and regulation of movements," *Neuropsychologia*, vol. 6, no. 1, pp. 90–91, Mar. 1968.

[14] A. Roby-Brami, A. Feydy, M. Combeaud, E. V. Biryukova, B. Bussel, and M. F. Levin, "Motor compensation and recovery for reaching in stroke patients," *Acta Neurol. Scandinavica*, vol. 107, no. 5, pp. 369–381, May 2003.

[15] J. Roh, W. Z. Rymer, E. J. Perreault, S. B. Yoo, and R. F. Beer, "Alterations in upper limb muscle synergy structure in chronic stroke survivors," *J. Neurophysiol.*, vol. 109, no. 3, pp. 768–781, Feb. 2013.

[16] V. C. K. Cheung *et al.*, "Muscle synergy patterns as physiological markers of motor cortical damage," *Proc. Nat. Acad. Sci. USA*, vol. 109, no. 36, pp. 14652–14656, Aug. 2012.

[17] D. J. Clark, L. H. Ting, F. E. Zajac, R. R. Neptune, and S. A. Kautz, "Merging of healthy motor modules predicts reduced locomotor performance and muscle coordination complexity post-stroke," *J. Neurophysiol.*, vol. 103, no. 2, pp. 844–857, Feb. 2010.

[18] L. Pellegrino, M. Coscia, M. Muller, C. Solaro, and M. Casadio, "Evaluating upper limb impairments in multiple sclerosis by exposure to different mechanical environments," *Sci. Rep.*, vol. 8, no. 1, p. 2110, Feb. 2018.

[19] D. S. Reisman, "Aspects of joint coordination are preserved during pointing in persons with post-stroke hemiparesis," *Brain*, vol. 126, no. 11, pp. 2510–2527, Nov. 2003.

[20] S. Ferrante *et al.*, "A personalized multi-channel FES controller based on muscle synergies to support gait rehabilitation after stroke," *Frontiers Neurosci.*, vol. 10, p. 425, Sep. 2016.

[21] L. H. Ting *et al.*, "Neuromechanical principles underlying movement modularity and their implications for rehabilitation," *Neuron*, vol. 86, no. 1, pp. 38–54, Apr. 2015.

[22] P. Otten, J. Kim, and S. Son, "A framework to automate assessment of upper-limb motor function impairment: A feasibility study," *Sensors*, vol. 15, no. 8, pp. 20097–20114, Aug. 2015.

[23] V. Tedim Cruz, V. F. Bento, D. D. Ribeiro, I. Araújo, C. A. Branco, and P. Coutinho, "A novel system for automatic classification of upper limb motor function after stroke: An exploratory study," *Med. Eng. Phys.*, vol. 36, no. 12, pp. 1704–1710, Dec. 2014.

[24] S. Patel *et al.*, "Tracking motor recovery in stroke survivors undergoing rehabilitation using wearable technology," in *Proc. Annu. Int. Conf. IEEE Eng. Med. Biol.*, Aug. 2010, pp. 6858–6861.

[25] C. P. Warlow *et al.*, *Stroke: Practical Management*. Hoboken, NJ, USA: Wiley, 2011.

[26] D. Tolani and N. I. Badler, "Real-time inverse kinematics of the human arm," *Presence: Teleoperators Virtual Environ.*, vol. 5, no. 4, pp. 393–401, Jan. 1996.

[27] C. Wang *et al.*, "Kinematic redundancy analysis during goal-directed motion for trajectory planning of an upper-limb exoskeleton robot," in *Proc. 41st Annu. Int. Conf. IEEE Eng. Med. Biol. Soc. (EMBC)*, Jul. 2019, pp. 5251–5255.

[28] T. Flash and N. Hogan, "The coordination of arm movements: An experimentally confirmed mathematical model," *J. Neurosci.*, vol. 5, no. 7, pp. 1688–1703, Jul. 1985.

[29] R. Shadmehr *et al.*, *The Computational Neurobiology of Reaching and Pointing: A Foundation for Motor Learning*. Cambridge, MA, USA: MIT Press, 2005.

[30] C. Li, S. Q. Zheng, and B. Prabhakaran, "Segmentation and recognition of motion streams by similarity search," *ACM Trans. Multimedia Comput., Commun., Appl.*, vol. 3, no. 3, p. 16, Aug. 2007.

[31] J. C. Platt, "Probabilistic outputs for support vector machines and comparisons to regularized likelihood methods," *Adv. Large Margin Classifiers*, vol. 10, no. 3, pp. 61–74, 1999.

[32] C. E. Metz, "Basic principles of ROC analysis," *Seminars Nucl. Med.*, vol. 8, no. 4, pp. 283–298, Oct. 1978.

[33] J. Benesty, J. Chen, Y. Huang, and I. Cohen, "Pearson correlation coefficient," in *Noise Reduction in Speech Processing*. Berlin, Germany: Springer, 2009, pp. 1–4.